Climatic Change (2022) 173: 22
https://doi.org/10.1007/s10584-022-03416-w

Extreme drought events diagnosed along the Yellow River and the adjacent area

Yongxiang Zhang[1] · Hongli Wang[2] · Xuemei Shao[2,3] · Jinbao Li[4] · Guoyu Ren[1,5]

Received: 12 March 2022 / Accepted: 26 July 2022 / Published online: 10 August 2022

Abstract

Drought is a major natural disaster that has long-lasting effects on economic and social activities in northern China and has regional distinctions in duration, severity, and spatial extent. In this study, tree-ring chronologies and historical archives in the Yellow River Basin and its surrounding areas are collected to investigate the extreme drought history and dynamic process of the two extreme drought events for the past ~ 200 years. Instead of reconstructing climate indicators, the tree index is directly employed here to partly overcome the high-frequency information loss during tree-ring-based reconstruction. The results show that identified drought history is improved significantly relative to the single indicator reconstruction, and drought events are highly consistent with historical recorded ones. Two prominent drought events in modern Chinese history are analyzed, namely the Ding-Wu Great Famine (1876–1879) and the extreme drought in northern China during the late-1920s. Unexpectedly, the most prestigious Ding-Wu Great Famine is lower than the extreme drought in the late-1920s in terms of drought duration, spatial extent, and intensity. Our research further reveals that the drought events recorded in the historical records could be very different from actual events due to the influence of political and other factors. The analysis of spatial dynamics indicates that the potential mechanisms of the two drought events are also different. This is confirmed by research based on reanalysis data that the Ding-Wu Great Famine was caused by a typical strong ENSO event, while the mechanism of the extreme drought in the late-1920s was more complicated.

Keywords Tree ring · Historical documents · Extreme drought · Identification

✉ Yongxiang Zhang
Helen.zyx@hotmail.com; zhangyx@cma.cn

1 National Climate Center, China Meteorological Administration, Beijing, China

2 Key Laboratory of Land Surface Pattern and Simulation, Institute of Geographic Sciences and Natural Resources Research, Chinese Academy of Sciences, Beijing, China

3 University of Chinese Academy of Sciences, Beijing, China

4 Department of Geography, The University of Hong Kong, Hong Kong SAR, China

5 Present Address: Department of Atmospheric Science, School of Environmental Studies, China University of Geosciences, Wuhan, China

1 Introduction

Drought, as the world's costliest natural disaster (Smith and Katz 2013; Wilhite 2000), has plagued civilizations throughout the course of human history. In the context of continued global warming (Allan et al. 2021), the frequency and intensity of some extreme climate events are rapidly increasing (Donat et al. 2016), especially the meteorological drought caused by reduced precipitation and increased temperatures over much of the globe (Grossiord et al. 2017). In particular, arid and semi-arid regions have experienced severe water stress (Allan and Soden 2008), with millions of people suffering crop failure and facing subsistence pressure (Haywood et al. 2013). The impacts of extreme drought events, or the so-called mega-droughts, can be multiplied by poor governance and then induce social unrest, famine and massive population fatality, economic collapse, and even dynasty subrogation (Hao et al. 2021). It is critical to improving our understanding of drought dynamics and impacts in the context of climate change.

However, drought is difficult to measure or even to define, which hinders accurate drought characterizations. Moreover, due to the lack of instrumental records, it is difficult to diagnose and distinguish whether a disaster is man-made or natural, which in turn makes it difficult to understand the mechanism of disaster occurrence. The demand for monitoring complicated drought conditions has prompted many efforts to develop drought indicators based on different applications, regions affected, and data availability (Heim Jr and Brewer 2012; Mishra and Singh 2010), which take into account a variety of hydroclimatic variables, such as precipitation, soil moisture, streamflow, snow, groundwater, evapotranspiration, and vegetation. Meanwhile, reliable prediction of drought onset, development, and recovery is an important step toward effective early warnings, which can be achieved through either statistical approaches to explore empirical relationships in historical records or dynamical approaches based mostly on state-of-the-art general circulation models. To improve the accuracy of future mega-drought projections, it is critical to strengthen our understanding of the mechanisms influencing the occurrence and magnitude of mega-droughts at different time scales. The relatively short instrumental records (typically 150 years or less) limit our understanding of natural climate variability, especially for extreme events like droughts which are by definition rare and thus under-sampled in modern observations. These constraints present challenges for drought attribution, including both internal variability and external forcing.

Hydroclimate reconstructions developed from proxy records (e.g., tree-rings, sediment cores, speleothems) are critical for addressing the weakness of "short instrumental records" by extending the record further back in time (Macumber et al. 2018; Morales et al. 2020; Tan et al. 2014). Currently, proxy-based drought reconstructions, combined with climate model simulations and proxy-system models, provide the possibility of developing estimates of past multivariate climate variability that capture and account for the non-climatic influences of proxy data (Cook et al. 2018). Tree-ring data are exactly dated and widespread over the mid-latitudes, which allow them to be statistically compared and calibrated with the instrumental observations in both space and time. Trees are naturally good records of extreme events, especially droughts. Tree-ring-based drought reconstructions have been widely used to better characterize and constrain the magnitude and processes of natural drought variability and contextualize recent trends (Davi et al. 2009). Instead of using the reconstruction index to depict the drought events, using the direct impact of the drought on tree radial growth could be a better way to reflect the severity of the drought (Meko et al. 1995). According to dendroecological studies (Gao et al. 2018; Meko et al. 1995), the trees could vary their response strategy to cope with extreme drought although their main limiting factor could be others. This provides another way to investigate the mega-droughts in history.

Yellow River Basin (YRB) is the birthplace of ancient Chinese civilization. However, affected by both summer monsoon and westerly, this area has been plagued by various drought disasters in history. Some of those extreme drought events, e.g., the Northern Chinese Famine of 1876–1879 (Ding-Wu Great Famine) (Zhao 1981) and the extreme drought in northern China in the late-1920s (Dong et al. 2010), had caused severe social upheaval. Some studies based on historical documents and other proxy data had tried to unveil the process and mechanism of these mega-droughts (Aceituno et al. 2009; Liang et al. 2003; Peng 2021; Zhang et al. 2011a). However, the lack of climatic records and deviations in literature constrain the understanding of the mechanisms of these extreme drought events, which has been a limiting factor for establishing an effective drought warning system in these drought-prone areas. Hereby, we apply a simple approach based on tree-ring data combined with literature reconstruction in the Yellow River basin to investigate the mega-droughts from a new perspective.

2 Data and methods

2.1 Study area

The YRB mainly refers to the mid-latitude regions of Eurasia from 96°E to 119°E and 32°N to 42°N (Fig. 1) (http://www.yrcc.gov.cn/). The Yellow River (YR) originates on the northeastern Qinghai-Tibet Plateau (TP), which is less affected by the monsoon; and then it flows through the Inner Mongolia Plateau, Loess Plateau, and North China Plain. Most areas of the YRB have an arid and semi-arid climate with fragile ecological environment. The uneven distribution of precipitation in the YRB and the inherent shortage of water resources make this region one of the areas prone to drought and flood disasters, especially extreme drought (Lu 1998). Our study area has been divided into three sub-regions, namely Y_{upper}, Y_{mid}, and Y_{down}, based on the geographic units and precipitation distribution. The Y_{upper} region narrows the upper stream of the YR to include only the northeastern TP, and extends to the Qilian Mountains. The Y_{mid} region is mainly located in the western part of the Loess Plateau, while the Y_{down} region encompasses the eastern Loess Plateau and the North China Plain. The entire study area is abbreviated as Y_{all}. According to the monthly meteorological data (China Meteorological Data Service Centre) of each sub-region from 1981 to 2010, the annual precipitation increased from 368 mm/year and 530 mm/year in the Y_{upper} and Y_{mid} regions to 670 mm/year in the Y_{down} region (Fig. 1b–d). The corresponding annual mean temperature are 3.35 °C, 10 °C, and 11.69 °C, respectively.

2.2 Proxy and climate data

Twenty-nine tree-ring-width chronologies were employed in this study, all of which were older than 1850 A.D. and the tree-ring radial growth was mainly limited by moisture (Table 1, nos. 1–29). All of these tree-ring chronologies were processed using standard techniques of dendrochronology (Cook and Kairiukstis 1990). To compensate for the scarcity of tree-ring data in the Y_{down} region that is heavily affected by intensive human activity, 1 tree-ring-based (Table 1, no. 30) and 5 literature-based precipitation or moisture

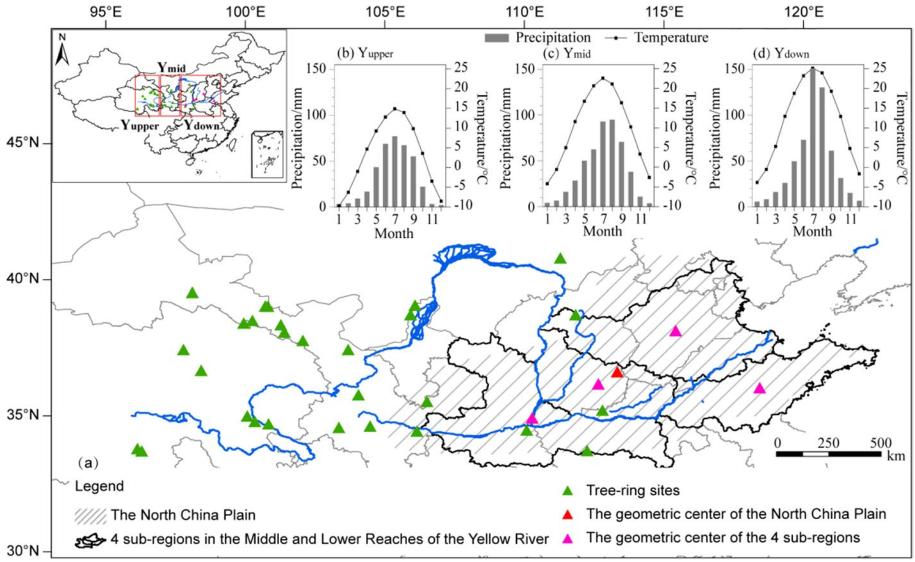

Fig. 1 The study area with data sites and climate conditions. Green triangles represent the tree-ring sites adopted in previous studies employed in this study. Purple and red triangles represent the geographic center points of the four subregions and North China Plain respectively, where literature-based climate reconstruction areas are. The climographs b–d of the monthly mean temperature and total precipitation values of the three subregions during the period of 1981–2010. Y_{upper}, Y_{mid}, and Y_{down} are marked on the location map

reconstructions were also included (Table 1, nos. 31–35). Climate data were obtained from the Climatic Research Unit (CRU) Time-Series (TS) version 4.05 worldwide dataset available on a $0.5° \times 0.5°$ grid (Harris et al. 2021), which were used to reveal the regional representativeness of proxy data. Moreover, gridded drought index such as self-calibrating Palmer Drought Severity Index (Barichivich et al. 2021) and 1-month Standardized Precipitation-Evapotranspiration Index (CSIC SPEI, Vicente-Serrano et al. 2010) were also obtained from the KNMI Climate Explorer (Trouet and Oldenborgh 2013) (http://climexp.knmi.nl).

2.3 Regional extreme drought diagnosing in proxy data

Z-score normalization was applied to all series to make all data comparable. Principal component analysis (PCA) was applied to identify distinct growth patterns within large datasets. In addition, spatial correlations between climate data (monthly temperature and precipitation) and proxy data were used to examine the representativeness of proxy data for drought events. To better depict the most impactful drought period on regional agricultural production, PDSI and SPEI were also selected to analyze the spatial correlation with each PC1 series during 1950–1995. Spatial correlation analysis was conducted using the KNMI Climate Explorer. Drought years were identified as those with values < mean-1σ (σ = standard deviation), and extreme drought year as those with values < mean-2σ. A period of two or more consecutive years was considered drought periods and extreme drought periods, respectively. Moreover, historical literatures were used for cross-validation. This article will focus on the two extreme drought events: the Ding-Wu Great Famine (DWGF) and the

Table 1 Information of tree-ring chronologies and reconstructed precipitation/dry–wet indices

No	Area	Region	Code	Latitude/longitude	Period	References/contributors
1	Y_{upper}	Qumalai	QML	33.80°N/96.13°E	1480–2002	Qin et al. (2003)
2		Zhiduo	ZHD	33.72°N/96.28°E	1374–2002	Qin et al. (2003)
3		Zhongtie	DQL	35.00°N/100.07°E	1178–2004	Peng et al. (2007)
4		Yangyu	YYAH	34.80°N/100.34°E	1399–2002	Peng et al. (2007)
5		Hebeidong	HHBMH	34.71°N/100.83°E	1800–2004	Peng et al. (2007)
6		Delingha	DLH5	37.45°N/97.79°E	711–2003	Shao et al. (2006)
7		Wulan	WL4	36.68°N/98.42°E	900–2001	Shao et al. (2006)
8		Jiuquan	DHS	39.55°N/98.10°E	1768–2009	Chen et al. (2011)
9		Sidalong	SDL	38.42°N/99.94°E	1785–2005	Zhang et al. (2011b)
10		Dayekou	DYK	38.52°N/100.25°E	1780–2005	Zhang et al. (2011b)
11		dongdashan	DDS	39.04°N/100.81°E	1779–2005	Zhang et al. (2011b)
12		Xidahe	XDH	38.09°N/101.40°E	1770–2005	Zhang et al. (2011b)
13		Xiyinghe	XYH	37.78°N/102.06°E	1288–2000	Yongxiang Zhang
14		Zhangye	TLC	39.05°N/100.72°E	1737–2010	Chen et al. (2013b)
15		Shandan	DHG	38.36°N/101.27°E	1768–2006	Chen et al. (2010)
16	Y_{mid}	Changling Mts	CLS	37.45°N/103.68°E	1644–2008	Chen et al. (2012)
17		Xinglong Mts	YDG	35.78°N/104.05°E	1807–2010	Chen et al. (2015)
18		Dieshan Mts	DS	34.58°N/103.35°E	1637–2013	Fang et al. (2013)
19		Guiqing Mts	GQM	34.63°N/104.47°E	1618–2005	Fang et al. (2010)
20		Shimen Mts	SMS	34.45°N/106.15°E	1666–2008	Chen et al. (2013a)
21		Kongtong Mts	KTS	35.55°N/106.51°E	1618–2009	Fang et al. (2012)
22		Suyukou	SYK	38.73°N/105.92°E	1700–1999	Yongxiang Zhang
23		Beisi	BSI	39.08°N/106.08°E	1739–1999	Yongxiang Zhang
24	Y_{down}	Huashan	HSW	34.48°N/110.08°E	1359–2005	Shao and Wu (1994)
25		Huashan	HSE	34.48°N/110.08°E	1458–2005	Shao and Wu (1994)
26		Huashan	HSS	34.48°N/110.08°E	1512–2005	Shao and Wu (1994)
27		Lamadong	LMD	40.81°N/111.29°E	1567–2017	Mingqi Li
28		Shiren Mts	YS	33.73°N/112.25°E	1801–2016	Peng et al. (2020)
29		Southern Taihang Mts	THS	35.21°N/112.8°E	1510–2013	Zhang et al. (2017)
30		Luya Mts. *	LY02	38.73°N/111.83°E	1600–2000	Yi et al. (2010)
31		North China Plain**		34–40°N/105–125°E	-133–1995	Zheng et al. (2006)
32		Hebei Region*			1736–2000	Hao et al. (2008)
33		Jinnan Region*			1736–2000	Hao et al. (2008)
34		Weihe Region*			1736–2000	Hao et al. (2008)
35		Shandong Region*			1736–2000	Hao et al. (2008)

*Represent this series is reconstructed precipitation; **represent this series is reconstructed dry–wet index

extreme drought in northern China in the late-1920s, which is also known as the Minguo extreme drought (MGED).

3 Results

3.1 Data representativeness of the moisture change over regions

Based on PCA method, the PC1 series over 1807–1995 explained 23.4%, 38.3%, 43.2%, and 36.4% of Y_{all}, Y_{upper}, Y_{mid}, and Y_{down}, respectively. The spatial correlations between the four PC1 series and monthly climate factors show that tree growth positively correlated with precipitation (negative with temperature) in September of the previous year and the early growing season of the current year (mainly April to June) within a large spatial range (Fig. S1–S5 in the Online Supplementary Information). The spatial correlation between each PC1 series and April to June precipitation during 1950–1995 showed that Y_{all} PC1 is significantly and positively correlated with early growing season precipitation in most parts of the study area (Fig. 2a). Y_{down} PC1 has a higher correlation coefficient (Fig. 2d) and the Y_{mid} PC1 has a relatively broader spatial representation, but the correlation coefficient is lower than Y_{down} region (Fig. 2c). The Y_{upper} region (Fig. 2b) significantly related to precipitation is limited to tree-ring sampling sites. Moreover, the spatial correlation patterns with SPEI were highly consistent with the precipitation ones and similar to the PDSI ones with slight difference (Fig. S6–S7 in the Online Supplementary Information). All results indicate that this data set can depicted regional and sub-regional moisture and drought pattern.

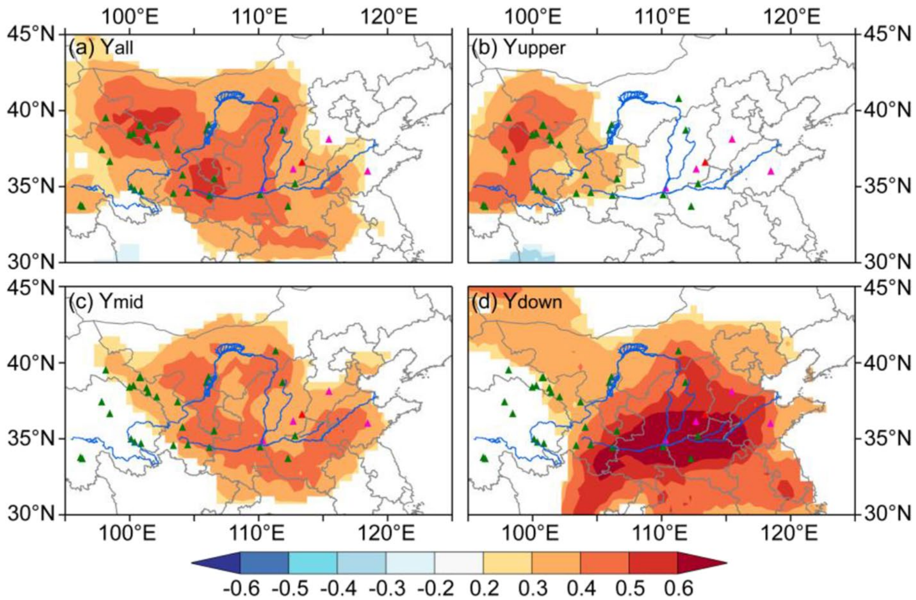

Fig. 2 Spatial correlations between the gridded April to June precipitation (CRU TS 4.05) and the PC1 series of (**a**) Y_{all}, (**b**) Y_{upper}, (**c**) Y_{mid}, and (**d**) Y_{down} during 1950–1995. The identification of triangles is the same as in Fig. 1. The colored areas indicate the areas with significant correlations ($p < 0.1$)

3.2 Major drought events in the Yellow River Basin

The four PC1 series are shown in Fig. 3a. The mean value of each PC1 series is 0, and the standard deviation (1σ) of the PC1 is 2.86 (Y_{all}), 2.40 (Y_{upper}), 1.86 (Y_{mid}), and 2.09 (Y_{down}). For the Y_{all} area, 29 drought years and 8 extreme drought years have been identified during the past two centuries (Table 2). The three prominent drought periods lasting more than 2 years are 1861–1862, 1918–1919, and 1926–1932. Furthermore, most of the drought years from the late 1920s to the early 1930s reached an extreme level. For the three sub-regions, the Y_{mid} region has the most drought years, up to 35 years, which may be related to the transitional geographic location of this region. Compared to the Y_{mid} region, the Y_{down} and Y_{upper} regions have relatively few drought years, which are 30 and 26 years respectively. The extreme droughts mainly occurred between 1870 and 1930 in the Y_{down} region, and after the 1900s in the Y_{mid} region, and evenly distributed throughout the study period in the Y_{upper} region. In addition, the extreme drought in the late 1920s was prominent in all sub-regions.

3.3 The comparison between DWGF and MGED

These two extreme drought events have different features over our study area as shown in Fig. 3b, c. In terms of spatial extent, the MGED or late-1920s extreme drought was well recorded in the three subregions, but the most severe drought occurred in the Y_{upper}.

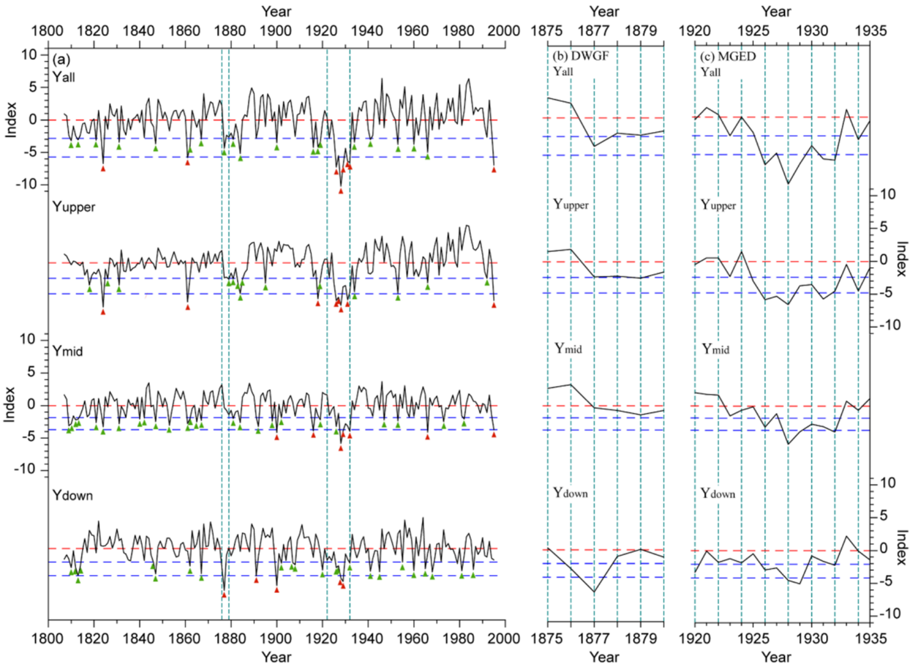

Fig. 3 (**a**) The PC1 series and details of (**b**) DWGF and (**c**) MGED. The DWGF and MGED are delineated by green vertical lines annually. The red and blue horizontal dashed lines indicate the mean, mean-1σ, and mean-2σ, respectively. The green and red triangles indicate the drought years and extreme drought years, respectively

Table 2 Listing of the drought years

Region	Drought (< mean-1σ)	Extreme drought (< mean-2σ)
Y_{all}	1810, 1813, 1821, 1824, 1831, 1847, **1861–1862**, 1867, 1877, 1881, 1884, 1900, 1916, **1918–1919**, **1926–1932**, 1934, 1941, 1953, 1960, 1966, 1995	1824, 1861, 1926, **1928–1929**, **1931–1932**, 1995
Y_{upper}	1818, 1824, 1826, 1831, 1861, 1879, 1881, 1883–1885, 1895, **1918–1919**, **1925–1932**, 1934, 1953, 1966, 1992, 1995	1824, 1861, 1918, **1926–1928**, 1931, 1995
Y_{mid}	**1809–1810**, **1812–1813**, 1821, 1824, 1831, 1840, 1842, 1847, 1853, **1861–1862**, 1865, 1867, 1881, 1884, 1892, 1898, 1900, 1902, 1916, 1919, 1926, **1928–1932**, 1947, 1953, 1966, 1973, 1982, 1995	1900, 1916, **1928–1929**, 1932, 1966, 1995
Y_{down}	1810, 1812–1814, **1846–1847**, 1862, 1867, **1876–1877**, 1891, 1900, 1902, **1907–1908**, 1920, **1926–1929**, 1932, 1941, 1945, 1955, 1960, 1965, 1968, 1979, 1981, 1986	1877, 1891, 1900, **1928–1929**

Bold texts indicate these drought/extreme drought periods lasting more than 2 years

However, DWGF was more like a regional drought event limited to North China compared to the MGED, with the former happening only in the Y_{down} region. For duration, MGED is far greater than DWED. The MGED began earlier at the Y_{upper} from 1924 and lasted until 1932, with the Y_{upper} lasting longer than the other two areas. In terms of intensity, DWGF only experienced a severe drought in the Y_{down} region in 1877, and it was the severest of all the identified drought years during the study period. The DWGF developed rapidly into extreme drought in the Y_{down} region and then returned to normal quickly, whereas the MGED developed slowly and lasted much longer. All in all, MGED is severer than DWGF, which seems to be inconsistent with what is recorded in the historical literature which will be discussed in the following.

4 Discussion

4.1 The identification of drought events by tree-ring index

For drought information prior to the instrumental period, we have to rely on proxy indicators of climate. Tree ring better preserve both low- and high-frequency variations of climate, and the excellent high-frequency variability provides abundant evidence for studying climate extremes (Bräuning et al. 2016). Numerous studies have shown that extreme drought events recorded by tree rings are highly consistent with those recorded in the historical literature (Sun and Liu 2019; Zhang et al. 2011a). Drought events recorded in historical literatures and identified by tree rings were mutually validated. Furthermore, drought is definitely not a local phenomenon, but occurs on a considerable scale (Zhang 2010). Therefore, the drought and extreme drought years in Table 2 were investigated individually by searching local historical drought records and instrumental data, respectively. The results show that drought years identified in this study are reliable and can well characterize drought history, especially extreme drought events. For pre-1950, the agreement of extreme drought years was 100% in the three sub-regions; the agreement of drought years was about 86% in the Y_{upper} region and 100% in the Y_{mid} and Y_{down} regions (Table S1 in the Online Supplementary Information) (Ding 2008; Wen and Zhai 2005; Wen and Wang 2006; Wen and Xia 2007a, b; Yuan 1994; Zhang 2013; Zhang and Jiang 2004).

For the years after 1950, interannual precipitation variations in the tree sub-regions based on CRU gridded data (Harris et al. 2021) were performed (Fig. S8 in the Online Supplementary Information). The results show that in the Y_{down} region, the drought years 1965, 1968, 1981, and 1986 identified by proxy indicators were also detected by the analysis of instrumental data; for the Y_{mid} region, it was consistent only in 1982; however, there is no overlap in the Y_{upper} region. The inconsistency between the PCA series and the observational precipitation data may have been due to the fact that drought is usually caused by the variation of multi-variables rather than the decrease in precipitation. As for the extreme drought year 1966 in Y_{mid} region, we found that it was lower in 1965 based on instrumental results, which may be related to the lag effect of climate change on tree growth (Fritts 1976). Liu et al. (2017) pointed out that the drought lasted consecutive 11 months from May 1965 to March 1966 in the Loess Plateau. Moreover, in 1995, the summer grain in northern Shannxi and central-southern Ningxia was basically out of production due to drought (Wen and Zhai 2005; Wen and Xia 2007b). All of these concretely demonstrate that climatic information embedded in the tree-ring chronologies can provide qualitative measures of drought severity and fill the gaps where historical documents are lacking and insufficient.

4.2 What really happened behind the history records

Drought is one of the most serious climate disasters affecting the stability of agricultural society. However, historical documents and other materials, which are important ways to reconstruct historical droughts, often deviate from the actual climate disasters because of political factors, information inequity, and even the subjective perception bias of the recorder (Zheng et al. 2014). According to historical records, the DWGF, one of the most famous extreme droughts in Chinese history, started in 1876 and ended in 1879, has affected 160–200 millions of people, and caused more than 10 million deaths (Hao et al. 2010; Xia 1992; Zhao 1981). MGED is less famous than DWGF but also causing severe disasters (Li et al. 1994) and serious impacts (Chen et al. 2022). The question here is how exactly these two drought events are, and are they consistent with what has been described?

To better understand the dynamic process of these two extreme droughts, the spatial features of each drought event were demonstrated annually by the standardized values of each sample site. Figure 4 visualizes the differences between the two major drought events in terms of spatial extent, duration, and drought severity. During the DWGF (Fig. 4a), the drought first developed in the Y_{down} region, while the Y_{mid} and Y_{upper} regions were only a few scattered sample sites with negative values. In 1877, the drought had gradually extended from east to west (Zhou et al. 2019), and reached its peak. From 1878 to 1879, the drought eased in the Y_{down} region and continued to develop in the Y_{mid} and Y_{upper} regions. This dynamic evolution process was also verified by historical literature (Zhang and Liang 2010). Compared with DWGF, MGED developed more slowly and lasted longer (Fig. 4b). In the early 1920s, the drought was sporadic and divergent, and then expanded to surrounding areas year by year (Dong et al. 2010). From 1926, drought was found almost

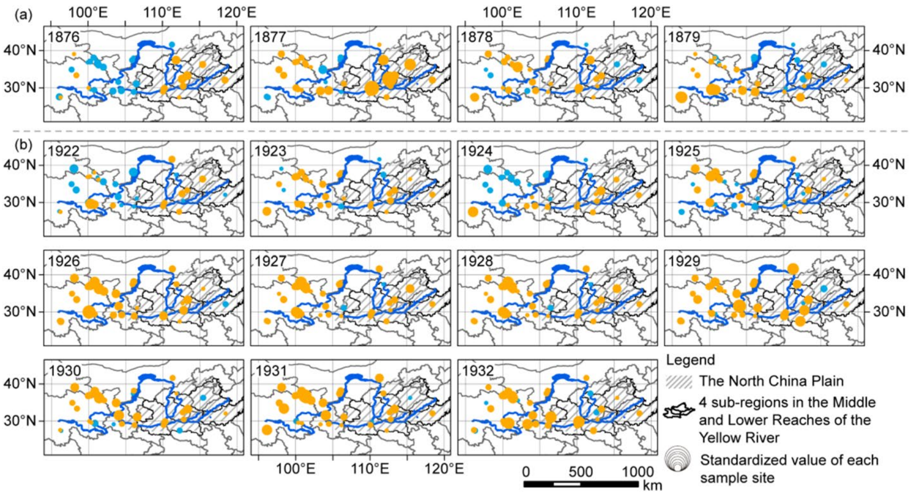

Fig. 4 The spatial distribution of standardized value of each sample site during DWGF and MGED.The size of circle indicates the standard value. Yellow means less than 0, blue means greater than 0

throughout the entire study, and reached its peak in 1928–1929, with the Y_{upper} region being the severest, and then gradually eased after 1932. Extreme drought disasters in agricultural societies often cause severe damage, while poor social management can exacerbate the impact of disasters (Zhai et al. 2020; Zhao 2008). The DWGF happened during the period of dynastic decline after the Opium War of the Qing Dynasty. Both the central government and the people were in a difficult time after the war. After the disaster, the social problems were superimposed and magnified each other, e.g., corrupt officials, lack of emergency management measures, and misappropriation of disaster relief funds (Xia 1992). It is more like a disaster management failure with complex social problem finally made the notorious consequences of DWGF, other than a few years early growing season moisture severe deficit. It nicely explains the inconsistency between the extent of drought recorded by tree rings and those recorded in the literature. Moreover, a valuable conclusion could be drawn that a combination of dendrochronology and historical records yields more useful information about past droughts than one or the other of these sources can provide alone.

4.3 The potential mechanism of these two extreme droughts

ENSO interacts closely with Asian monsoon dynamics, which in turn influence conditions over much of China (Lu 2005; Wang and Li 2004; Zhang et al. 1999). Statistical experience shows that in the El Niño year, or the sequent year, or in the summer when the El Niño episode is weakened, the rainfall pattern of southern flooding and northern drought often occurs in eastern China (Hao et al. 2008, 2010; Zhao 1996). The comparison between the identified drought/extreme drought years and reconstructed ENSO series (Gergis and Fowler 2009) showed that about 73% and 68% of the drought/extreme drought years correspond to the occurrence of El Niño in the Y_{upper} and Y_{mid} regions, and even higher in the Y_{down} region, reaching 80% (Table S2). Previous studies also indicated that major El Niño episode that started by the end of 1876 and peaked during the 1877–1878 boreal winter contributed significantly to the DWGF (Hao et al. 2010; Kiladis and Diaz 1986). The periodic analysis (Fig. S9b in the Online Supplementary Information) also clearly indicates that the significant cycle in the Y_{down} area in the late 1870s is 2–4 years, which coincided with ENSO. Moreover, the positive SST anomalies of the tropical Pacific Ocean spread and intensified throughout the east tropical Pacific during 1877–1878 (Fig. 6 in Kang et al. 2013). The most dramatic impacts of this typical El Niño event were associated with intense and long-lasting droughts in Asia, Brazil, America, Africa, and other regions (Aceituno et al. 2009; Singh et al. 2018). In addition, the DWGF was also driven by a positive Pacific Decadal Oscillation (PDO) (Hao et al. 2021).

In contrast, the mechanisms affecting MGED are more complex. From the comparison with El Niño, it can be found that the occurrence of El Niño had an impact on the MGED, but other potential mechanisms should be considered. Fig. S9a shows that the climate variability in the study area may be related to the 30–60-year periodicals, which may be partially in association with the PDO. PDO exhibits considerable influence on summer precipitation in eastern China (D'Arrigo and Wilson 2006), by modulating the strength of the summer monsoon and the location of the subtropical high. In this study, we compared the PC series with the reconstructed monthly PDO index (April to June) (Huang et al. 2017) and found that the PDD was significantly negatively correlated with all PC series (Y_{all}: $r=-0.211$, $p=0.012$; Y_{mid}: $r=-0.224$, $p=0.007$; Y_{down}: $r=-0.231$, $p=0.006$), except Y_{upper} region ($r=-0.107$, $p=0.204$). The "warm" PDO regimes dominated from 1925–1946, coinciding with the persistent drought of the late 1920s to the early 1930s. Similar correlation results were also found with April to June NAO (Jones et al. 1997), which was positively correlated with all PC series (Y_{all}: $r=0.222$, $p=0.003$; Y_{upper}: $r=0.188$, $p=0.013$; Y_{mid}: $r=0.197$, $p=0.009$), except for the Y_{down} region ($r=0.123$, $p=0.109$). A previous study has shown that the negative phase of summer North Atlantic Oscillation (SNAO) may be a contributing driver of extreme drought in northern China (Du et al. 2020). This suggests that ENSO and the joint impact of PDO and NAO may also have been responsible for the decadal dry anomaly during the event (Luo et al. 2019). In addition, this severe drought was an anomalous dry period accompanied by a decadal warm phase under the background of a century-scale warming (Qian et al. 2007).

5 Conclusions

In this study, 29 tree-ring chronologies, 1 tree-ring-based reconstructed precipitation series, and 5 historical literature–based reconstructed precipitation/dry–wet indices were employed to analyze drought events over the past ~ 200 years along the Yellow River Basin and its adjacent areas. Principal component analysis was used to extract common signals and the results show that the proxies, mainly tree-ring chronologies, can effectively characterize the drought history at large scales. Identified drought events in our study area have been verified by historical records and meteorological observations. The two prominent drought events, Ding-wu Great Famine (DWGF: 1876–1879) and extreme drought during the late-1920s in northern China (MGED), had different spatial propagation as well as drought duration, spatial extent, and intensity. The DWGF was less severe than the MGED in our study, which is contrary to their fame as recorded in the historical literatures. The mechanism indicates that tree-ring data can better facilitate the interpretation of the extreme drought mechanism by capturing the real situation of the drought events.

Supplementary Information The online version contains supplementary material available at https://doi.org/10.1007/s10584-022-03416-w.

Acknowledgements The authors also would like to thank Prof. Feng Chen, Prof. Keyan Fang, Prof. Zhixin Hao, Dr. Mingqi Li, Prof. Jianfeng Peng, Prof. Ningsheng Qin, Dr. Liang Yi, Dr. Yong Zhang, and Prof. Jingyun Zheng for data support (sort alphabetically by last name).

Funding This work was supported by the National Key Research and Development Program of China (grant no. 2018YFA0605601), the Strategic Priority Research Program of the Chinese Academy of Sciences (grant no. XDA20070101), and the National Natural Science Foundation of China (grant no. 41572353, 41401228, 41690113).

Data availability Data will be made available on reasonable request.

Declarations

Competing interests The authors declare no competing interests.

References

Aceituno P, Del Rosario PM, Solari ME, Martínez A, Poveda G, Falvey M (2009) The 1877–1878 El Niño episode: associated impacts in south America. Clim Change 92(3–4):389–416. https://doi.org/10.1007/s10584-008-9470-5

Allan RP, Soden BJ (2008) Atmospheric warming and the amplification of precipitation extremes. Science 321(5895):1481–1484. https://doi.org/10.1126/science.1160787

Allan RP, Hawkins E, Bellouin N, Collins B (2021) IPCC, 2021: summary for policymakers. In: Masson-Delmotte V, Zhai PM, Priani A et al (eds) Climate Change 2021: The Physical Science Basis. Contribution of Working Group I to the Sixth Assessment Report of the Intergovernmental Panel on Climate Change. Cambridge University Press, London, pp 3–32

Barichivich J, Osborn T, Harris I, van der Schrier G, Jones P (2021) Monitoring global drought using the self-calibrating Palmer Drought Severity Index. B Am Meteorol Soc 102(8):S68–S70

Bräuning A, De Ridder M, Zafirov N, García-González I, Dimitrov DP, Gärtner H (2016) Tree-ring features: indicators of extreme event impacts. IAWA J 37(2):206–231. https://doi.org/10.1163/22941932-20160131

Chen F, Yuan YJ, Wei WS, Yu SL, Fan ZA, Zhang RB, Shang HM, Zhang TW (2010) Reconstruction of Annual Precipitation in Shandan Based Tree-Ring since 1783A.D. Geogr Geo-information Sci 26(5):82–86

Chen F, Yuan YJ, Wei WS (2011) Climatic response of Picea crassifolia tree-ring parameters and precipitation reconstruction in the western Qilian Mountains, China. J Arid Environ 75(11):1121–1128. https://doi.org/10.1016/j.jaridenv.2011.06.010

Chen F, Yuan YJ, Wen WS, Yu SL, Fan ZA, Zhang RB, Zhang TW, Shang HM (2012) Tree ring based reconstruction of precipitation in the Changling Mountains, China, since AD 1691. Int J Biometeorol 56(4):765–774. https://doi.org/10.1007/s00484-011-0431-8

Chen F, Yuan YJ, Wei WS, Fan ZA, Yu SL, Zhang TW, Zhang RB, Shang HM, Qin L (2013a) Reconstructed precipitation for the north-central China over the past 380 years and its linkages to East Asian summer monsoon variability. Quatern Int 283:36–45. https://doi.org/10.1016/j.quaint.2012.05.047

Chen F, Yuan YJ, Wei WS, Zhang RB, Yu SL, Shang HM, Zhang TW, Qin L, Wang HQ, Chen FH (2013b) Tree ring based annual precipitation reconstruction for the Hexi Corridor, NW China: consequences for climate history on and beyond the mid-latitude Asian continent. Boreas 42(4):1008–1021. https://doi.org/10.1111/bor.12017

Chen F, Wang HQ, Chen FH, Yuan YJ, Zhang RB (2015) Tree-ring reconstruction of July-May precipitation (AD 1816–2010) in the northwestern marginal zone of the East Asian summer monsoon reveals the monsoon-related climate signals. Int J Climatol 35(8):2109–2121. https://doi.org/10.1002/joc.4110

Chen XD, Tian FY, Su Y (2022) How did the late 1920s drought affect northern Chinese society? Weather and Climate Extremes 36:100451. https://doi.org/10.1016/j.wace.2022.100451

Cook ER, Kairiukstis LA (1990) Methods of dendrochronology: applications in the environmental sciences. Kluwer Academic Publishers, Dordrecht

Cook BI, Mankin JS, Anchukaitis KJ (2018) Climate change and drought: from past to future. Curr Clim Chang Rep 4(2):164–179. https://doi.org/10.1007/s40641-018-0093-2

D'Arrigo R, Wilson R (2006) On the Asian expression of the PDO. Int J Climatol 26(12):1607–1617. https://doi.org/10.1002/joc.1326

Davi NK, Jacoby GC, D'Arrigo RD, Baatarbileg N, Li JB, Curtis AE (2009) A tree-ring-based drought index reconstruction for far-western Mongolia: 1565–2004. Int J Climatol 29(10):1508–1514. https://doi.org/10.1002/joc.1798

Ding YH (2008) China meteorological disaster code. China Meteorological Press, Beijing

Donat MG, Lowry AL, Alexander LV, Gorman PAO, Maher N (2016) More extreme precipitation in the world`s dry and wet regions. Nat Clim Chang 5(6):508–513. https://doi.org/10.1038/nclimate2941

Dong AX, Liu YP, Li XP, Bai HZ (2010) Characteristics and influence of the extreme drought event lasting eleven years (1922–1932) in the Yellow River Valley. J Arid Meteorol 28(3):270–278. https://doi.org/10.3969/j.issn.1006-7639.2010.03.005

Du YB, Zhang J, Zhao SW, Chen HS (2020) Impact of the eastward shift in the negative-phase NAO on extreme drought over Northern China in summer. J Geophys Res: Atmos 125(16):e2019J-e32019J. https://doi.org/10.1029/2019JD032019

Fang KY, Gou XH, Chen FH, D'Arrigo R, Li JB (2010) Tree-ring based drought reconstruction for the Guiqing Mountain (China): linkages to the Indian and Pacific Oceans. Int J Climatol 30(8):1137–1145. https://doi.org/10.1002/joc.1974

Fang KY, Gou XH, Chen FH, Liu CZ, Davi N, Li JB, Zhao ZQ, Li YJ (2012) Tree-ring based reconstruction of drought variability (1615–2009) in the Kongtong Mountain area, northern China. Global Planet Change 80–81:190–197. https://doi.org/10.1016/j.gloplacha.2011.10.009

Fang KY, Frank D, Gou XH, Liu CZ, Zhou FF, Li JB, Li YJ (2013) Precipitation over the past four centuries in the Dieshan Mountains as inferred from tree rings: an introduction to an HHT-based method. Global Planet Change 107(4):109–118. https://doi.org/10.1016/j.gloplacha.2013.04.010

Fritts HC (1976) Tree rings and climate. Academic Press, New York

Gao S, Liu RS, Zhou T, Fang W, Yi CX, Lu RJ, Zhao X, Luo H (2018) Dynamic responses of tree-ring growth to multiple dimensions of drought. Glob Change Biol 24(11):5380–5390. https://doi.org/10.1111/gcb.14367
Gergis JL, Fowler AM (2009) A history of ENSO events since AD 1525: implications for future climate change. Clim Change 92(3–4):343–387. https://doi.org/10.1007/s10584-008-9476-z
Grossiord C, Sevanto S, Dawson TE, Adams HD, Collins AD, Dickman LT, Newman BD, Stockton EA, McDowell NG (2017) Warming combined with more extreme precipitation regimes modifies the water sources used by trees. New Phytol 213(2):584–596. https://doi.org/10.1111/nph.14192
Hao ZX, Zheng JY, Ge QS (2008) Precipitation cycles in the middle and lower reaches of the Yellow River (1736–2000). J Geog Sci 18(1):17–25. https://doi.org/10.1007/s11442-008-0017-5
Hao ZX, Zheng JY, Wu GF, Zhang XZ, Ge QS (2010) 1876–1878 severe drought in North China: facts, impacts and climatic background. Chin Sci Bull 55(26):3001–3007. https://doi.org/10.1007/s11434-010-3243-z
Hao ZX, Bai MX, Xiong DY, Liu Y, Zheng JY (2021) Severe droughts of 1876–1878 in North China and possible causes. Clim Change 167(7):1–15. https://doi.org/10.21203/rs.3.rs-161952/v1
Harris I, Jones PD, Osborn TJ (2021) CRU TS4.05: Climatic Research Unit (CRU) time-series (TS) version 4.05 of high-resolution gridded data of month-by-month variation in climate (Jan. 1901- Dec. 2020). https://catalogue.ceda.ac.uk/uuid/c26a65020a5e4b80b20018f148556681. Accessed 5 Mar 2021
Haywood JM, Jones A, Bellouin N, Stephenson D (2013) Asymmetric forcing from stratospheric aerosols impacts Sahelian rainfall. Nat Clim Chang 3(7):660–665. https://doi.org/10.1038/nclimate1857
Heim RR Jr, Brewer MJ (2012) The global drought monitor portal: the foundation for a global drought information system. Earth Interact 16(15):1–28. https://doi.org/10.1175/2012EI000446.1
Huang BY, Thorne PW, Banzon VF, Boyer T, Chepurin G, Lawrimore JH, Menne MJ, Smith TM, Vose RS, Zhang HM (2017) NOAA extended reconstructed sea surface temperature (ERSST), version 5. NOAA Natl Cent Environ Inf 30:8179–8205
Jones PD, Jonsson T, Wheeler D (1997) Extension to the North Atlantic Oscillation using early instrumental pressure observations from Gibraltar and south-west Iceland. Int J Climatol: J R Meteorol Soc 17(13):1433–1450. https://doi.org/10.1002/(SICI)1097-0088(19971115)17:13%3c1433::AID-JOC203%3e3.0.CO;2-P
Kang SY, Yang B, Qin C, Wang JL, Shi F, Liu JJ (2013) Extreme drought events in the years 1877–1878, and 1928, in the southeast Qilian Mountains and the air-sea coupling system. Quatern Int 283:85–92. https://doi.org/10.1016/j.quaint.2012.03.011
Kiladis GN, Diaz HF (1986) An analysis of the 1877–78 ENSO episode and comparison with 1982–83. Mon Weather Rev 114(6):1035–1047. https://doi.org/10.1175/1520-0493(1986)114%3c1035:AAOTEE%3e2.0.CO;2
Li WH, Chen X, Liu YD, Xia MF (1994) The top ten famine in recent China. Shanghai People's Press, Shanghai
Liang EY, Shao XM, Kong ZC, Lin JX (2003) The extreme drought in the 1920s and its effect on tree growth deduced from tree ring analysis: a case study in North China. Ann for Sci 60(2):145–152. https://doi.org/10.1051/forest:2003007
Liu YF, Yuan ZH, Li WZ, Kong W, Zhang L, Wu L (2017) Extreme and persistent analysis of drought-flood variation in the Loess Plateau during 1961–2013. Geogr Res 36(2):345–360. https://doi.org/10.11821/dlyj201702012
Lu CH (1998) Characteristics of drought and flooding hazards in the reaches of Yellow River. J Arid Land Resour Environ 12(1):2–7
Lu RY (2005) Interannual variation of North China rainfall in rainy season and SSTs in the equatorial eastern Pacific. Chin Sci Bull 50(18):2069–2073. https://doi.org/10.1007/BF03322803
Luo M, Feng JM, Xu ZF, Wang YL, Dan L (2019) Evaluating the performance of five twentieth-century reanalysis datasets in reproducing the severe drought in northern China during the 1920s–1930s. Theoret Appl Climatol 137(1):187–199. https://doi.org/10.1007/s00704-018-2591-5
Macumber AL, Patterson RT, Galloway JM, Falck H, Swindles GT (2018) Reconstruction of Holocene hydroclimatic variability in subarctic treeline lakes using lake sediment grain-size end-members. Holocene 28(6):845–857. https://doi.org/10.1177/0959683617752836
Meko D, Stockton CW, Boggess WR (1995) The tree-ring record of severe sustained drought. J Am Water Resour Assoc 31(5):789–801. https://doi.org/10.1111/j.1752-1688.1995.tb03401.x
Mishra AK, Singh VP (2010) A review of drought concepts. J Hydrol 391(1–2):202–216. https://doi.org/10.1016/j.jhydrol.2010.07.012
Morales MS, Cook ER, Barichivich J et al (2020) Six hundred years of South American tree rings reveal an increase in severe hydroclimatic events since mid-20th century. Proc Natl Acad Sci 117(29):16816–16823. https://doi.org/10.1073/pnas.2002411117

Peng YB (2021) Possible underlying mechanisms of severe decadal droughts in arid central asia during the last 530 years: results from the last millennium climate reanalysis Project Version 2.0. J Geophys Res: Atmos 126(5):e2020J-e33409J. https://doi.org/10.1029/2020JD033409

Peng JF, Gou XH, Chen FH, Zhang YX, Liu PX, Zhang Y, Fang KY (2007) Horizontal variations of climatic response of Qilian Juniper (Juniperus przewalskii) in the Anyemaqen Mountains. Acta Geogr Sin 62(7):742–752. https://doi.org/10.3321/j.issn:0375-5444.2007.07.007

Peng JF, Li JB, Yang L, Li JR, Huo JX (2020) A 216-year tree-ring reconstruction of April-July relative humidity from Mt. Shiren, central China. Int J Climatol 40(14):1–12. https://doi.org/10.1002/joc.6565

Qian WH, Lin X, Zhu YF, Xu Y, Fu JL (2007) Climatic regime shift and decadal anomalous events in China. Clim Change 84(2):167–189. https://doi.org/10.1007/s10584-006-9234-z

Qin NS, Shao XM, Jin LY, Wang QC, Zhu XD, Wang ZY, Li JB (2003) Climate change over southern Qinghai Plateau in the past 500 years recorded in Sabina Tibetica tree rings. Chin Sci Bull 48(19):2068–2072. https://doi.org/10.3321/j.issn:0023-074X.2003.19.013

Shao XM, Wu XD (1994) Radial growth of Huashan pine and its response to climate. J Chin Geogr 4(3/4):88–102

Shao XM, Liang EY, Huang L, Wang LL (2006) A reconstructed precipitation series over the past millennium in the Northeastern Qaidam Basin. Adv Clim Chang Res 2(3):122–126. https://doi.org/10.3969/j.issn.1673-1719.2006.03.006

Singh D, Seager R, Cook B, Cane M, Ting MF, Cook E, Davis M (2018) Climate and the global famine of 1876–78. J Clim 31(23):9445–9467. https://doi.org/10.1175/JCLI-D-18-0159.1

Smith AB, Katz RW (2013) US billion-dollar weather and climate disasters: data sources, trends, accuracy and biases. Nat Hazards 67(2):387–410. https://doi.org/10.1007/s11069-013-0566-5

Sun CF, Liu Y (2019) Tree-ring-based drought variability in the eastern region of the Silk Road and its linkages to the Pacific Ocean. Ecol Indic 96:421–429. https://doi.org/10.1016/j.ecolind.2018.09.032

Tan LC, An ZS, Huh CA, Cai YJ, Shen CC, Shiau LJ, Yan LB, Cheng H, Edwards RL (2014) Cyclic precipitation variation on the western Loess Plateau of China during the past four centuries. Sci Rep 4:6381. https://doi.org/10.1038/srep06381

Trouet V, Oldenborgh GJV (2013) Research tools KNMI Climate Explorer: a web-based research tool for high-resolution paleoclimatology. Tree-Ring Res 69(1):3–13. https://doi.org/10.3959/1536-1098-69.1.3

Vicente-Serrano SM, Beguer IAS, Lopez-Moreno JI (2010) A multiscalar drought index sensitive to global warming: the standardized precipitation evapotranspiration index. Journal of Climate 23(7):1696–1718. https://doi.org/10.1175/2009JCLI2909.1

Wang B, Li T (2004) East Asian monsoon-ENSO interactions. In: Chang CP (ed) East Asian Monsoon. World Scientific, Singapore, pp 177–212

Wen KG, Wang S (2006) China Meteorological Disaster Code (Qinghai). China Meteorological Press, Beijing

Wen KG, Xia PM (2007a) China Meteorological Disaster Code (Gansu). China Meteorological Press, Beijing

Wen KG, Xia PM (2007b) China Meteorological Disaster Code (Ningxia). China Meteorological Press, Beijing

Wen KG, Zhai YA (2005) China Meteorological Disaster Code (Shaanxi). China Meteorological Press, Beijing

Wilhite DA (2000) Drought as a natural hazard: concepts and definitions. In: Wilhite DA (ed) Drought: A Global Assessment. Routledge, London, pp 3–18

Xia MF (1992) A study of Ding-Wu Disaster. Stud Qing Hist 1(4):83–91

Yi L, Yu HJ, Xu XY, Yao J, Su Q, Ge JY (2010) Exploratory precipitation in North-Central China during the past four centuries. Acta Geol Sin 84(1):223–229. https://doi.org/10.1111/j.1755-6724.2010.00184.x

Yuan L (1994) The history of drought and the famine in Northwestern China. The People's Publishing Company of Gansu Province, Lanzhou

Zhai XS, Fang XQ, Su Y (2020) Regional interactions in social responses to extreme climate events: a case study of the North China Famine of 1876–1879. Atmosphere 11(4):393. https://doi.org/10.3390/atmos11040393

Zhang DE (2010) Test of calibration on the paleoclimatic proxy data by using Chinese historical records. Adv Clim Chang Res 6(1):70–72. https://doi.org/10.3969/j.issn.1673-1719.2010.01.012

Zhang DE (2013) A compendium of Chinese meteorological records of the last 3000 years (Update). Jiangsu Education Publishing Ltd, Nanjing

Zhang DE, Jiang GM (2004) A compendium of Chinese meteorological records of the last 3000 years. Jiangsu Education Publishing Ltd, Nanjing

Zhang DE, Liang YY (2010) A long lasting and extensive drought event over China during 1876–1878. Adv Clim Chang Res 6(2):106–112. https://doi.org/10.3969/j.issn.1673-1719.2010.02.006
Zhang RH, Sumi A, Kimoto M (1999) A diagnostic study of the impact of El Niño on the precipitation in China. Adv Atmos Sci 16(2):229–241. https://doi.org/10.1007/BF02973084
Zhang Y, Shao XM, Yin ZY, Liang EY, Tian QH, Xu Y (2011a) Characteristics of extreme droughts inferred from tree-ring data in the Qilian Mountains, 1700–2005. Climate Res 50(2):141–159. https://doi.org/10.3354/cr01051
Zhang YX, Shao XM, Wilmking M (2011b) Dynamic relationships between Picea crassifolia growth and climate at upper treeline in the Qilian Mts., Northeast Tibetan Plateau, China. Dendrochronologia 29(4):185–199. https://doi.org/10.1016/j.dendro.2010.11.001
Zhang Y, Tian QH, Guillet S, Stoffel M (2017) 500-yr. precipitation variability in Southern Taihang Mountains, China, and its linkages to ENSO and PDO. Clim Change 144(3):419–432. https://doi.org/10.1007/s10584-016-1695-0
Zhao SY (1981) A brief introduction of Ding-Wu great famine. Acad Mon 25(2):65–68
Zhao ZG (1996) Impact of El Niño events on atmospheric circulations in the northern hemisphere and precipitation in China. Scientia Atmospherica Sinica 20(4):422–425
Zhao XH (2008) On the social order of the “Incredible Famina” in 1876–1879: based on the study of the local chronicals. J South China Normal Univ (Social Science Edition) 2:82–87
Zheng JY, Wang WC, Ge QS, Man ZM, Zhang PY (2006) Precipitation variability and extreme events in eastern China during the past 1500 years. Terr Atmos Ocean Sci 17(3):579–592. https://doi.org/10.3319/TAO.2006.17.3.579(A)
Zheng JY, Ge QS, Hao ZX, Liu HL, Man ZM, Hou YJ, Fang XQ (2014) Paleoclimatology proxy recorded in historical documents and method for reconstruction on climate change. Quat Sci 34(6):1186–1196. https://doi.org/10.3969/j.issn.1001-7410.2014.06.07
Zhou S, Wang YM, Chang JX, Guo AJ, Li ZY (2019) Research on spatio-temporal evolution of drought patterns in the Yellow River Basin. J Hydraul Eng 50(S):1–11. https://doi.org/10.13243/j.cnki.slxb.20190348